

Characterization of Calcium, Strontium, Barium and Lead Hydroxyapatites: X-ray Diffraction, Photoelectron, Extended X-ray Absorption Fine Structure and MAS NMR Spectroscopies

Shigeru Sugiyama,* Toshihiro Moriga, Hiromu Hayashi, and John B. Moffat†

Department of Chemical Science and Technology, Faculty of Engineering, The University of Tokushima, Minamijosanjima, Tokushima 770-8506

† Department of Chemistry and Guelph-Waterloo Centre for Graduate Work in Chemistry and Biochemistry, University of Waterloo, Waterloo, Ontario N2L 3G1, Canada

(Received June 7, 2000)

Calcium, strontium, barium and lead hydroxyapatites have been investigated by X-ray diffraction (XRD), X-ray photoelectron spectroscopy (XPS), extended X-ray absorption fine structure (XAFS) and solid state NMR. XPS analyses showed that the binding energies of P 2s or P 2p and O 1s of all hydroxyapatites, XRD of which matched to the corresponding JCPDS data, were essentially identical and were not influenced by those divalent cations. In contrast, it was revealed that the nearest neighbour distances between divalent cations and oxygen determined by XAFS and the chemical shifts of ^{1}H and ^{31}P NMR were strongly influenced by each divalent cation in hydroxyapatites.

Apatites are of interest to a wide variety of scientists for both fundamental and application purposes.[1–3] The most widely studied of these is calcium hydroxyapatite [$Ca_{10}(PO_4)_6(OH)_2$] which is of particular interest as the major constituent of bone. Calcium hydroxyapatite has a hexagonal structure constructed from columns of Ca and O atoms which are parallel to the hexagonal axis.[1] Three oxygen atoms of each PO_4 tetrahedron are shared by one column, with the fourth oxygen atom attached to a neighboring column. The hexagonal unit cell of hydroxyapatite contains 10 cations located on two sets of nonequivalent sites, 4 on site [1] and 6 on site [2]. The calcium ions on site [1] are aligned in columns, while those on site [2] are in equilateral triangles centered on the screw axes. The site-[1] cations are coordinated to six oxygen atoms belonging to different PO_4 tetrahedra and also to three oxygen atoms at a large distance. The site-[2] cations are found in cavities in the walls of the channels formed between the cations and O atoms. The hydroxide groups are situated in these channels and form an approximately triangular coplanar arrangement with the cations. Although hydroxyapatite has a number of characteristic properties, two of these are especially noteworthy. The structure is amenable to both cationic and anionic substitutions, although certain of the divalent cations, for example Mg^{2+}, can only be partially accommodated. However calcium can be completely replaced by barium, cadmium, lead and strontium with semiquantitative retention of the crystallographic structure.[4]

Although a plethora of the structural data is available for calcium hydroxyapatite, including the results from X-ray diffraction (XRD),[1,5,6] ^{31}P and ^{1}H MAS NMR[1,5,7–11] and X-ray absorption spectroscopy (XAFS)[12], relatively little such information is available where the cation is Sr^{2+}, Ba^{2+} and Pb^{2+}. Noteworthy exceptions apply to Pb^{2+} for which the results from X-ray[13] and neutron powder diffraction studies[14] have been reported.

The present work provides further structural data on calcium, strontium, barium and lead hydroxyapatites (CaHAp, SrHAp, BaHAp and PbHAp, respectively) from XRD, X-ray photoelectron spectroscopy (XPS), XAFS and ^{1}H and ^{31}P MAS NMR.

Experimental

Materials. All chemicals were of high purity and were used as supplied. Calcium hydroxyapatite was prepared from $Ca(NO_3)_2{\cdot}4H_2O$ (Wako Pure Chemicals, Osaka) and $(NH_4)_2HPO_4$ (Wako).[15,16] Strontium hydroxyapatite was similarly prepared from $Sr(NO_3)_2$ (Wako) and $(NH_4)_2HPO_4$.[17,18] Preparative details of CaHAp and SrHAp were as follows. $Ca(NO_3)_2{\cdot}4H_2O$ (78.83 g; 333.8 mmol) and $Sr(NO_3)_2$ (70.64 g; 333.8 mmol) were each dissolved in 300 ml of distilled water. Those solutions were adjusted to pH 11 by the addition of 25% ammonia solution (Wako) and then diluted to 600 ml, respectively. Into those Ca^{2+}- and Sr^{2+}-containing solutions was dropped, slowly with vigorous stirring at room temperature, a solution of 25.27 g (191.4 mmol) and 29.38 g (222.5 mmol) of $(NH_4)_2HPO_4$ in 500 ml of distilled water, respectively, both of which similarly had been brought to pH 11 with ammonia and thereafter diluted to 800 ml. Therefore apparent atomic ratios of Ca/P and Sr/P in the preparative step were adjusted to 1.74 and 1.50 for CaHAp and SrHAp, respectively. Voluminous precipitates formed from both solutions, those were further boiled for 10 min with stirring. The resulting solids were filtered, washed to pH 7 with distilled water and then dried in air at 373 K overnight. Barium hydroxyapatite was prepared from $Ba(OH)_2{\cdot}8H_2O$ (Wako) and H_3PO_4 (Wako).[19,20] Lead hydroxyapatite was prepared from H_3PO_4 (Wako) and $Pb(NO_3)_2{\cdot}5PbO$,[4,21] the latter of which was obtained through dehydration of lead(II) hydroxide nitrate.

Preparative details of BaHAp and PbHAp were described in our previous papers.[20,21] All hydroxyapatites thus obtained were calcined at 773 K for 3 h in air.

Characterization. The cation/phosphorus (atom/atom) ratios in each of the hydroxyapatites were determined in aqueous HNO_3 solutions by inductively coupled plasma (ICP) spectrometry (ICPS-5000, Shimadzu). The surface areas were measured with a conventional BET nitrogen adsorption apparatus (Shibata P-700). Surface analyses by XPS were carried out with a Perkin-Elmer Model 5500 spectrometer using Mg $K\alpha$ radiation. The binding energies were corrected using 285 eV for C 1s as an internal standard. Argon-ion etching of the sample was carried out at 4 kV for 1 min with a sputtering rate estimated as ca. 12.5 nm min^{-1} for SiO_2. Powder XRD patterns were recorded with Rigaku RINT 2500X diffractometer using monochromatized Cu $K\alpha$ radiation. Patterns were recorded over the range 5–60 degrees. XAFS near the Ca *K*- and Ba L_3-edge were measured (2.5 GeV) with a storage ring current of 320 mA at the High Energy Research Organization. The X-rays were monochromatized with Si(111) double monochromator and higher order harmonics were eliminated by a focusing double mirror system. The absorption spectra were observed using ionization chamber in a transmission mode at the BL-7C station. The photon energy was scanned in the range 3.7–4.9 and 5.0–5.6 keV for the Ca *K*- and Ba L_3-edges. Following the standard procedure, the XAFS interference function $\chi(k)$ was extracted from the absorption spectra. The radial structure functions $\phi(r)$ were obtained from the Fourier transform of $k^3\chi(k)$. The back scattering amplitude and the phase shift function of Teo and Lee[22] or McKale et al.[23] were used. For the curve-fitting, the range of interest for $\phi(r)$ was filtered with a Hamming window function, and transformed back to k space, $\chi'(k)$. Curve-fitting calculation for $\chi'(k)$[24] was performed over k range of 3–10 and 3–9 $Å^{-1}$ for the Ca *K*- and Ba L_3-edges, respectively. As a reference, commercially available $CaCO_3$ and $BaCO_3$ were also analyzed with XAFS. XAFS analyses of Sr *K*- and Pb L_3-edges of SrHAp and PbHAp, respectively, were investigated similarly as described in our previous paper.[25] ^1H NMR (one pulse) and ^{31}P CP/MAS NMR was obtained with a Bruker ADVANCE DSX300, with an external reference of $[(CH_3)_3Si]_4Si$ at 0.236 ppm and $NH_4H_2PO_4$ at 1.00 ppm, respectively, at room temperature and a spinning rate of 25 and 5 kHz, respectively.

Results and Discussion

The X/P (X = Ca, Sr, Ba and Pb) ratios, as obtained from composition of X and P, both determined by ICP, for the various hydroxyapatites prepared as stoichiometric compounds, show significant deviations from the expected stoichiometry (Table 1). This is not surprising in view of the well-known difficulty in preparing the stoichiometric materials.[1] Since the four cations carry the same change, the variation of the stoichiometry shown in Table 1 must tentatively be attributed to the cationic size differences. It has been suggested from structure fields that calcium could be totally replaced by ions in the fluorapatite and chlorapatite lattices provided that the replacing species have radii less than 1.35 Å,[26] a condition apparently satisfied in the present work. The existence of cation-rich hydroxyapatites, particularly with Ca^{2+} as the cation, has been reported as early as 1940[27] but were thought to be biphasic systems. However more recent studies showed that the separate phase, originally believed to be $Ca(OH)_2$, was absent at least up to Ca/P = 1.75.[28] Although no definitive explanation can be advanced, the cation-rich preparations with Pb^{2+} and Ba^{2+} in the present work may contain sufficient numbers of hydroxide groups to counterbalance the excess cationic charge.

Table 1. Composition of Hydroxyapatites

Cation (X)	Ionic radius/Å	X/wt%	P/wt%	X/P[a)]
Ca^{2+}	0.99	38.07	18.76	1.57
Sr^{2+}	1.12	56.87	13.35	1.51
Ba^{2+}	1.20	73.65	8.83	1.88
Pb^{2+}	1.34	84.62	6.49	1.95

a) From ICP.

X-ray photoelectron spectroscopy was performed on the hydroxyapatite samples (Table 2). The values obtained for the various binding energies (BE) of the cations are in good agreement with those expected.[29] The BE for oxygen shows little or no shifts with changes in the cations. The value found for the cation/phosphorous and the O/P ratios may be compared with those measured by ICP (Table 1). For the stoichiometric hydroxyapatite these ratios are expected to be 1.67 and 4.33, respectively. For CaHAp the Ca/P value in the absence of etching is in agreement with that from ICP, while O/P is larger than expected. Although a number of formulations have been proposed for calcium-deficient hydroxyapatite, perhaps the most generally recognized is $Ca_{10-x}(HPO_4)_x(PO_4)_{6-x}(OH)_{2-x}$ in which the decreased positive charge is balanced by a reduction in the hydroxide ions and a conversion of a portion of the phosphate ion contents to hydrogenphosphate ions. Thus, as the calcium-deficiency increases (x increases), the total number of oxygen atoms should decrease. However, as seen in Table 2, the O/P ratio is higher than expected. Etching produces higher than expected values for both Ca/P and O/P. For Sr-deficient SrHAp, the measured value of Sr/P is higher than expected, while that for O/P, based on the nonstoichiometric formula is approximately equal to that calculated. With both BaHAp and PbHAp, the values of Ba/P and Pb/P, after etching, are approximately equal to those obtained from ICP, while the O/P values are high, possible due to increased number of hydroxide groups required to balance the surplus positive charge. It should be noted that no C 1s signal other than that due to contamination carbon from the apparatus and no shoulder in O 1s spectra were observed in XPS of those hydroxyapatites, indicating that carbonate species and hydroxide group other than that in hydroxyapatites may not be significant.

The XRD patterns of CaHAp, SrHAp, BaHAp and PbHAp are in agreement with reference patterns $Ca_{10}(PO_4)_6(OH)_2$ [JCPDS 9-0432], $Sr_{10}(PO_4)_6(OH)_2$ [JCPDS 33-1348], $Ba_{10}(PO_4)_6(OH)_2$ [JCPDS 36-0272] and $Pb_{10}(PO_4)_6(OH)_2$ [JCPDS 8-0259], respectively, although some noncrystallinity was evident in CaHAp and SrHAp (Fig. 1). Similar XRD patterns of those hydroxyapatites reveals that the structure continues to be hexagonal. It should be noted that the noncrystallinity decreases with increasing ionic radius of divalent cations.

XAFS analyses have been applied to provide information on

Table 2. Surface Area and the Results of XPS Analyses of Hydroxyapatites

	S.A.[a)]/$m^2\ g^{-1}$	Binding energy/eV			Atomic Ratio	
		M[b)]	O 1s	P 2s or P 2p[c)]	M/P	O/P
CaHAp	77.0	351.0	531.4	190.8	1.59	4.80
		(350.4	531.4	190.8	2.16	5.45)
SrHAp	61.1	280.0	531.5	191.1	1.68	4.07
		(279.9	531.6	191.0	2.19	4.31)
BaHAp	13.5	88.6	532.0	134.1	1.24	6.55
		(87.8	532.2	134.4	1.89	5.16)
PbHAp	6.4	413.9	531.1	190.5	1.54	5.12
		(412.3	531.2	190.7	1.99	5.11)

a) Surface area. b) Ca $2p_{1/2}$ for M = Ca, Sr $3p_{1/2}$ for M = Sr, Ba $4d_{5/2}$ for M = Ba, and Pb $4d_{5/2}$ for M = Pb, respectively. c) P 2s for CaHAp, SrHAp and PbHAp and P 2p for BaHAp.
Values in parentheses were those after argon-ion etching for 1 min.

the bond distances and the environments of each cation. The X-ray absorption near-edge structure (XANES) spectra near Ca *K*- and Ba L_3-edges of the fresh CaHAp and BaHAp are shown in Figs. 2(A) and 3(A), respectively. Figures 2(B) and 3(B) show the Fourier transform of the XAFS oscillation around the Ca *K*- and Ba L_3-edges of CaHAp and BaHAp, respectively. Phase shifts are not corrected in these spectra. It should be noted that the shapes of the Fourier transforms of CaHAp is essentially identical to that of the hydroxyapatite prepared with calcium acetate and disodium hydrogenphosphate.[30] The strongest peak in each spectrum corresponds to the nearest-neighbour distance Ca–O and Ba–O, respectively. The reliability of the phase shift and amplitude functions are tested at approximately the nearest distance by fitting the observed XAFS of each hydroxyapatite. Figures 2(C) and 3(C) show the optimum curve fitting around the Ca *K*- and Ba L_3-edges of CaHAp and BaHAp, in which solid lines represent the experimental data and the closed circles represent the calculated results. The results of the curve-fitting analyses for CaHAp and BaHAp are described in Table 3 together with those for SrHAp and PbHAp. The nearest neighbour distances between divalent cation and oxygen in CaHAp, SrHAp and BaHAp were approximately 2.40, 2.51 and 2.73 Å, approximately proportional to the cationic radii. It should be noted that the relatively large electronegativity of Pb (1.8) in comparison with that of Ca (1.0), Sr (1.0) and Ba (0.9) may be reflected in the shorter metallic radius of Pb (1.75 Å) contrasted with that of Ca (1.97 Å), Sr (2.15 Å) and Ba (2.17 Å). However, the Pb–O distance (2.14–2.38 Å, depending on Pb/P) did not follow the aforementioned proportionality with cationic radius. It has been reported for the sto-

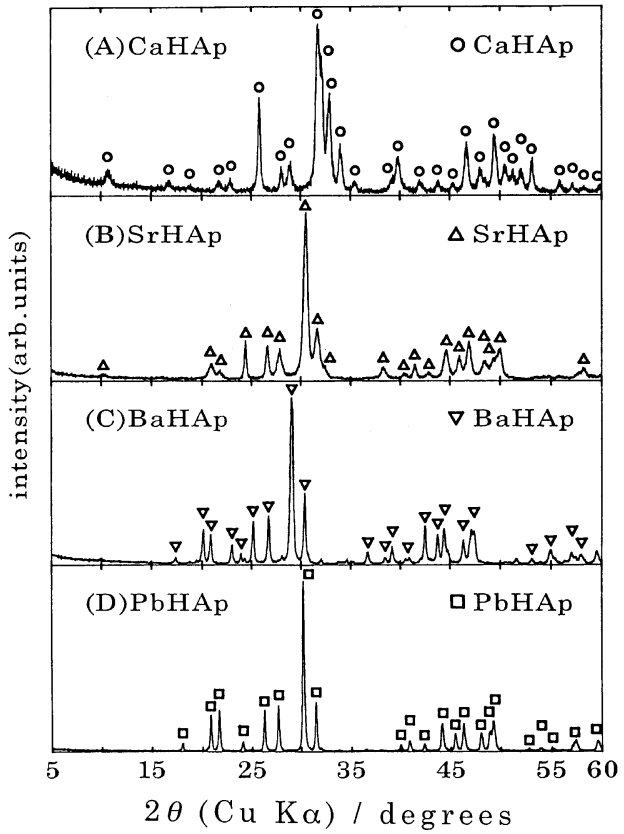

Fig. 1. XRD patterns of CaHAp, SrHAp, BaHAp and PbHAp.

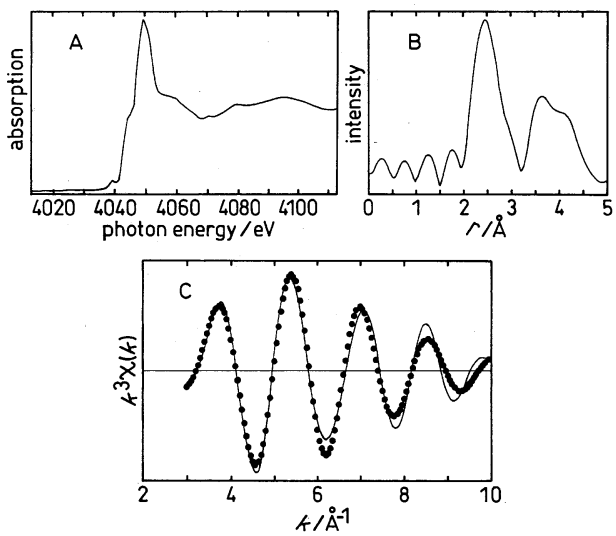

Fig. 2. XANES spectra (A), Fourier transformation of k^3-weighted XAFS oscillation (B) and the curve-fitting near Ca *K*-edge (C) measured at 300 K of CaHAp. Solid line in (C), experimental data; closed circles in (C), calculated values.

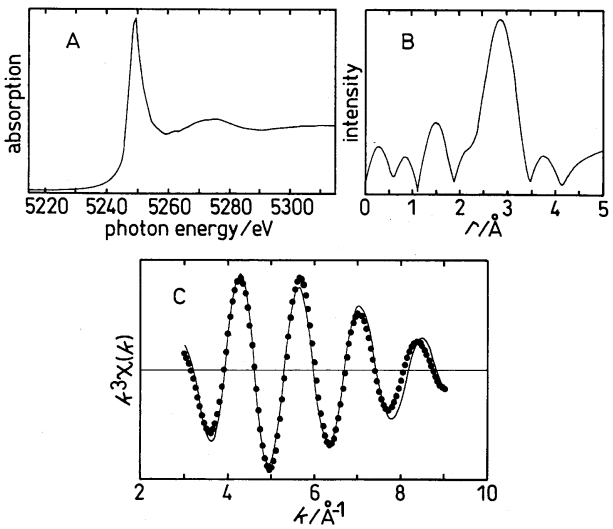

Fig. 3. XANES spectra (A), Fourier transformation of k^3-weighted XAFS oscillation (B) and the curve-fitting near Ba L_3-edge (C) measured at 300 K of BaHAp. Solid line in (C), experimental data; closed circles in (C), calculated values.

ichiometric PbHAp (Pb/P = 1.67) that the nearest neighbour distance of Pb–O estimated with the Rietvelt method by Bruckner et al.[13] and with neutron powder diffraction by Kim et al[14] was approximately 2.54 and 2.45 Å, respectively, apparently proportional to the cationic radius. In contrast, Mathew et al.[31] reported for $Pb_8K_2(PO_4)_6$ that the Pb–O distance in the equatorial plane was 2.56–2.67 Å, while that in the axial position was 2.24 Å, the latter of which was attributed to covalent bonding.

To provide further structural information, the solid state ^{1}H and ^{31}P NMR of hydroxyapatites have been observed (Fig. 4). The chemical shifts are summarized in Table 4. A single ^{31}P resonance at 2.8 ppm, which can be assigned to PO_4^{3-} ions in CaHAp,[7] was observed in the NMR spectrum of CaHAp (Fig. 4 (A)) together with weak sidebands at 44.4 and –38.8 ppm (not shown), indicating only slight distortion of the PO_4^{3-} ions from the undistorted tetrahedral symmetry.[7] The existence of only chemical shift demonstrates that the three crystallographically nonequivalent PO_4^{3-} ions in the unit cell have very similar environments.[1,32] Other workers have reported a shift of 2.9 ppm for crystalline CaHAp, presumably stoichiometric but without analytical data and 3.0 ppm for a calcium deficient (Ca/P = 1.50) CaHAp.[10,11] A sharp resonance with a chemical shift of 0.01 ppm in the ^{1}H NMR spectrum was assigned to structural OH^- ions and a resonance at 5.2 ppm to surface adsorbed water (Fig. 4(A) and Table 4). However, in view of the similarity of the isotropic chemical shift of adsorbed water and that of acid phosphate groups as well as the calcium-deficient stoichiometry in the present CaHAp, the ^{1}H NMR signal may alternatively be considered as arising from hydroxide and hydrogenphosphate groups.[11] Other workers have previously reported only one signal, at 0.8 ppm, for the apparent stoichiometric CaHAp, and an additional signal at 7 ppm originating from the hydrogenphosphate groups in the calcium-deficient (Ca/P = 1.50) CaHAp.[10] It should be noted that the sharp ^{1}H NMR resonance consists of two overlapping signals which may result from the existence of two different sites for the hydroxide group.[10,33] Although ^{31}P and ^{1}H NMR data have not been reported previously for the Sr, Ba and Pb hydroxyapatites, nevertheless the ^{31}P chemical shifts (Fig. 4 and Table 4) can be analogously assigned to the PO_4^{3-} ions. It is of interest to note that these values correlate inversely with the stoichiometry of the hydroxyapatites and the ionic radii of the cations (Tables 1 and 4). Similarly the ^{1}H signals of the aforementioned hydroxyapatites can be assigned to hydroxide groups and surface water and/or HPO_4^{2-}. ^{1}H NMR data can be employed to provide semiquantitative assessments of acidity.[34–38] The ^{1}H NMR chemical shift of hydroxide groups has been suggested as a measure of the acid strength[34–37] and a linear correlation between the deprotonation energy and the chemical shift of hydroxide groups has been demonstrated from quantum chemical calculations.[38] For purposes of comparison it can be noted that the proton chemical shifts for the SiOH hydroxy groups in H-Y and H-ZSM-5 zeolites are 2.0 and 2.1 ppm, respectively.[35] The positive value for the proton chemical shift of PbHAp as ob-

Table 3. Results of Curve-Fitting Analyses for Hydroxyapatites

	M/P[a)]	R_{M-O}[b)]/Å	N[c)]	σ[d)]/Å	E_0[e)]/eV	R[f)]/%	Ref.
CaHAp	1.57	2.40	6.3	0.133	9.57	19.3	Present
$CaCO_3$		2.37	6	0.121	9.31	3.2	Present
CaHAp	1.51–1.65	2.40					30
CaHAp	1.53–1.72	2.37–2.41					40
SrHAp	1.51	2.52	10.1	0.125	5.75	20.5	Present
SrHAp	1.60–1.74	2.51–2.52					Present
SrHAp	1.61–1.73	2.50-2.52					25, 41
BaHAp	1.88	2.73	4.2	0.138	10.77	18.7	Present
$BaCO_3$		2.75	6	0.133	9.76	8.3	Present
BaHAp	1.92–2.01	2.72–2.74					Present
PbHAp	1.72	2.18	7.3	0.124	−12.42	9.1	21
Pb–SrHAp		2.14–2.38 (for Pb–O)					25, 41

a) M = Ca, Sr, Ba or Pb. b) Distance. c) Coordination number. d) Debye–Waller (like) factor. e) Increment of threshold energy. f) Reliability factor.

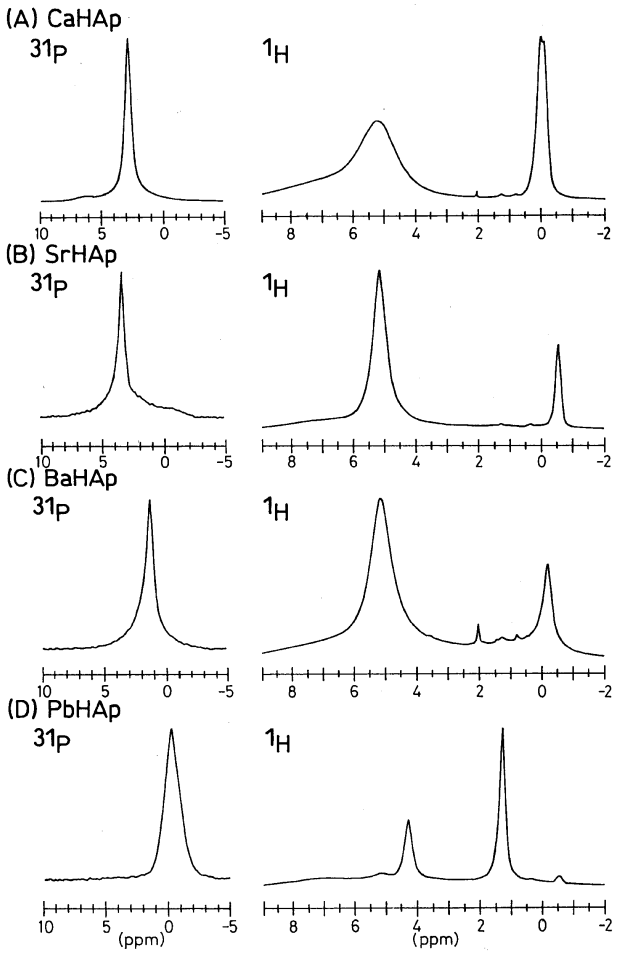

Fig. 4. ^{31}P and ^{1}H NMR of fresh CaHAp, SrHAp, BaHAp and PbHAp.

Table 4. Chemical Shift (ppm) in Hydroxyapatites

	^{31}P	^{1}H
CaHAp	2.8[a)]	−0.1; 5.2
SrHAp	3.4[a)]	−0.5; 5.2
BaHAp	1.3[a)]	−0.2; 5.1
PbHAp	0.3[a)]	1.3; 4.3

a) as well as weak side bands.

tained in the present work suggests that this material is acidic whereas the negative values found for the remaining hydroxyapatites may tentatively be interpreted as indicative of bases, observations which are in qualitative agreement with the catalytic properties of these hydroxyapatites in the conversion of methane.[39]

In the field of apatite chemistry, it has sometimes been mentioned that XRD analyses are not sufficient for the study, particularly on fine structure changes in hydroxyapatite. The present study suggests that XAFS and MAS NMR may be possible procedures for the structural analyses of hydroxyapatites.

The authors are grateful for grants to Shigeru Sugiyama as an overseas researcher at the University of Waterloo from the Japanese Ministry of Education Science, Sports and Culture and to John B. Moffat from the Natural Science and Engineering Research Council of Canada. This work has been performed under the approval of the Photon Factory Program Advisory Committee (97G030).

References

1 J. C. Elliott, "Structure and Chemistry of the Apatites and Other Calcium Orthophosphate," Elsevier, Amsterdam (1994).

2 P. W. Brown and B. Constantz, "Hydroxyapatite and Related Materials," CRC Press, Boca Raton (1994).

3 C. L. Kibby and W. K. Hall, "Surface Properties of Calcium Phosphates," in "The Chemistry Biosurfaces, Vol. 2," ed by M. L. Hair, Dekker, New York (1972).

4 A. Bigi, M. Gandolfi, A. Ripamonti, N. Roveri, and S. A. Thomas, *J. Chem. Soc., Dalton Trans.*, **1991**, 2883.

5 J. Arends, J. Christoffersen, M. R. Christoffersen, H. Eckert, B. O. Fowler, J. C. Heughevaert, G. H. Nancollos, J. P. Yesinowski, and S. J. Zawacki, *Crystal Growth*, **84**, 515 (1987).

6 M. Vallet-Regi, L. M. Rodrigues-Lorenzo, and A. J. Salina, *Solid State Ionics*, **101**, 1279 (1997).

7 W. P. Rothwell, J. S. Waugh, and J. P. Yesinoeski, *J. Am. Chem. Soc.*, **102**, 2637 (1980).

8 J. Tropp, N. C. Blumenthal, and J. S. Waugh, *J. Am. Chem. Soc.*, **105**, 22 (1983).

9 J. P. Yesinowski and H. Eckert, *J. Am. Chem. Soc.*, **109**, 6274 (1987).

10 J. L. Miquel, L. Facchini, A. P. Legrand, X. Marchardise, P. Lecouffe, M. Chanavaz, M. Donazyan, C. Rey, and J. Lemaitre, *Clinical Mater.*, **5**, 115 (1990).

11 J. L. Miquel, L. Facchini, A. D. Legrand, C. Rey, and J. Lemaitre, *Colloid and Surface*, **45**, 427 (1990).

12 J. E. Harries, D. W. L. Hukins, and S. S. Hasnain, *J. Phys. C: Solid State Phys.*, **19**, 6859 (1986).

13 S. Bruckner, G. Lusvardi, L. Menabue, and M. Saladini, *Inorg. Chim. Acta*, **236**, 209 (1995).

14 J. Y. Kim, B. A. Hunter, R. R. Fenton, and B. J. Kennedy, *Aust. J. Chem.*, **50**, 1061 (1997).

15 E. Hayek and H. Newesely, *Inorg. Snyth.*, **7**, 63 (1963).

16 S. Sugiyama, T. Minami, H. Hayashi, M. Tanaka, N. Shigemoto, and J. B. Moffat, *J. Chem. Soc., Faraday Trans.*, **92**, 293 (1996).

17 T. Ishikawa, H. Saito, and K. Kandori, *J. Chem. Soc., Faraday Trans.*, **88**, 2937 (1992).

18 Y. Matsumura, S. Sugiyama, H. Hayashi, N. Shigemoto, K. Saitoh, and J. B. Moffat, *J. Mol. Catal.*, **92**, 81 (1994).

19 A. Yasukawa, M. Kidokoro, K. Kandori, and T. Ishikawa, *J. Coll. Interface Sci.*, **191**, 407 (1997).

20 S. Sugiyama, T. Nakanishi, H. Hayashi, and J. B. Moffat, *Phosphorus Res. Bull.*, **8**, 23 (1998).

21 S. Sugiyama, T. Nakanishi, T. Ishimura, T. Moriga, H. Hayashi, N. Shigemoto, and J. B. Moffat, *J. Solid State Chem.*, **143**, 296 (1999).

22 B. K. Teo and P. A. Lee, *J. Am. Chem. Soc.*, **101**, 2815 (1979).

23 A.G. McKale, B. W. Veal, A. P. Paulikas, S. K. Chan, and G. S. Knapp, *J. Am. Chem. Soc.*, **110**, 3763 (1988).

24 H. Sakane, T. Miyanaga, I. Watanabe, N. Matsubayashi, S.

Ikeda, and Y. Yokoyama, *Jpn. J. Appl. Phys.*, **32**, 4641 (1993).

25 S. Sugiyama, T. Moriga, M. Goda, H. Hayashi, and J. B. Moffat, *J. Chem. Soc., Faraday Trans.*, **92**, 4305 (1996).

26 E. R. Kreidler and F. A. Hummel, *Am. Miner.*, **55**, 170 (1970).

27 S. Eisenberger, A. Lehrman, and W. D. Turner, *Chem. Rev.*, **26**, 257 (1940).

28 G. Bonel, J. -C. Heughebaert, M. Heughebaert, J. L. Lacout, and A. Leburgle, *Ann. Acad. Sci.*, **523**, 115 (1988).

29 H. Siegbahn, "ESCA Studies of Electronic Structure and Photoionization in Gases," U. Uppsala (1974).

30 S. Sugiyama, T. Yasutomi, T. Moriga, H. Hayashi, and J. B. Moffat, *J. Solid State Chem.*, **142**, 319 (1999).

31 M. Mathew, W. E. Brown, M. Austin, and T. Negas, *J. Solid State Chem.*, **35**, 69 (1980).

32 J. C. Elliott, P. E. Makie, and R. A. Young, *Science*, **180**, 1055 (1973).

33 M. I. Kay, R. A. Young, and S. A. Posner, *Nature*, **204**, 1050 (1964).

34 H. Pfeifer, "Acidity and Basicity," Kluwer, Dondrecht (1994), p.255.

35 H. Pfeifer, "NMR basic Principles and Progress," Springer, Berlin (1994), p.31.

36 E. Brunner and H. Pfeifer, *Z. Phys. Chemie*, **192**, 77 (1995).

37 E. Brunner, J. Karger, M. Koch, H. Pfeifer, H. Sachsenroder, and B. Staudte, *Stud. Surf. Sci. Catal.*, **105**, 463 (1997).

38 U. Fleischer, W. Kutzelnigg, A. Bleiber, and J. Sauer, *J. Am. Chem. Soc.*, **115**, 7833 (1993).

39 S. Sugiyama, K. Abe, H. Hayashi, and J. B. Moffat, *Catal. Lett.*, **57**, 161 (1999).

40 S. Sugiyama, T. Minami, T. Moriga, H. Hayashi, K. Koto, M. Tanaka, and J. B. Moffat, *J. Mater. Chem.*, **6**, 459 (1996).

41 S. Sugiyama, Y. Iguchi, H. Nishioka, T. Minami, T. Moriga, H. Hayashi, and J. B. Moffat, *J. Catal.*, **176**, 25 (1998).